ISSN: 1410-8917
Jurnal Kimia Sains & Aplikasi
e-ISSN: 2597-9914

Jurnal Kimia Sains dan Aplikasi 29 (4) (2026): 252-264

Jurnal Kimia Sains dan Aplikasi
Journal of Scientific and Applied Chemistry

Journal homepage: http://ejournal.undip.ac.id/index.php/ksa

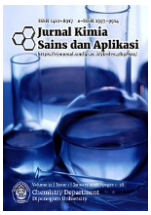

Synthesis of Polyethylene Glycol-Modified Salicylaldehyde–Chitosan Schiff Base and Its Antibacterial Assay

Umi Shofiyatun Ni'mah, Kamilia Hijriani Zain, Ngadiwiyana, Purbowatiningrum Ria Sarjono, Ismiyarto *

Chemistry Department, Faculty of Sciences and Mathematics, Diponegoro University, Jl. Prof. Soedarto, SH., Tembalang, Semarang, Indonesia

* Corresponding author: ismiyarto@live.undip.ac.id

https://doi.org/10.14710/jksa.29.4.252-264

Article Info

Article history:

Received: 20th January 2026
Revised: 09th March 2026
Accepted: 01st April 2026
Online: 25th May 2026

Keywords:
Chitosan; Schiff base; Salicylaldehyde; Polyethylene glycol; Crosslinking; Antibacterial activity

Abstract

Antibacterial materials are essential for inhibiting the growth of pathogenic microorganisms, and chitosan has received considerable attention due to its intrinsic antibacterial properties, biocompatibility, and biodegradability. However, the limited hydrophilicity and moderate mechanical strength of pristine chitosan restrict its broader application. In this study, chitosan was chemically modified through Schiff base formation with salicylaldehyde, followed by modification with polyethylene glycol (PEG), to enhance its physicochemical properties while maintaining detectable antibacterial performance. The objectives of this research were to synthesize Salicylaldehyde–chitosan Schiff base and PEG-modified Salicylaldehyde–chitosan Schiff base, to characterize their structural and physical properties, and to evaluate their antibacterial performance. The molecular weight of chitosan was determined by viscometry, and the degree of deacetylation was evaluated by Fourier transform infrared (FTIR) spectroscopy. The chitosan used exhibited a molecular weight of 147,926 g/mol and a degree of deacetylation of 67%. Schiff base formation was carried out by refluxing chitosan with salicylaldehyde at 60°C for 3 hours, using various molar ratios. The highest degree of substitution (68.75%) and yield (41.08%) were obtained, with the moderate yield attributed to incomplete conversion and material loss during purification steps. Structural confirmation was achieved through FTIR and UV–Vis spectroscopy by the appearance of characteristic imine (C=N) absorption bands. Subsequent modification with PEG at room temperature for 24 hours yielded 40.49%. The PEG-modified material exhibited significantly enhanced hydrophilicity, as indicated by a swelling ratio of 333.33% and a reduced contact angle of 63.04°. Antibacterial activity evaluated by the disc diffusion method showed inhibition zones of 9 mm against *Escherichia coli* and 10 mm against *Staphylococcus aureus*, which are modestly higher than those of the solvent control under the tested conditions. These results suggest that PEG modification improves the hydrophilicity of the chitosan-based Schiff base material while maintaining measurable antibacterial activity, indicating potential for further development in antimicrobial and biomedical materials.

1. Introduction

Bacteria are ubiquitous in the environment and can exert both beneficial and harmful effects. While certain bacterial species play important roles in ecological balance and industrial processes, pathogenic bacteria are responsible for a wide range of infectious diseases, particularly in individuals with compromised immune systems [1]. One effective strategy to reduce bacterial contamination and infection is the application of antibacterial materials that inhibit bacterial growth or induce bacterial cell death. Antibacterial agents can be classified as bacteriostatic, which suppress bacterial

proliferation, or bactericidal, which directly kill bacterial cells [2].

Chitosan, a linear polysaccharide derived from the partial deacetylation of chitin, has attracted considerable attention as an antibacterial material. Structurally, chitosan consists of β-(1→4)-linked D-glucosamine and N-acetyl-D-glucosamine units and is recognized as the second most abundant natural polysaccharide after cellulose. Chitosan exhibits several advantageous properties, including biodegradability, biocompatibility, non-toxicity, and broad-spectrum antimicrobial activity against bacteria, fungi, and yeast [3, 4]. Due to these properties, chitosan has been widely explored for applications in wound dressings [5, 6], food packaging and preservation [7], and antibacterial textiles [8].

Despite its promising antibacterial properties, the practical application of chitosan is limited by its poor mechanical strength and restricted solubility under neutral and basic conditions [9]. To overcome these limitations, various chemical modification strategies have been developed to improve the physicochemical properties of chitosan. These modifications are commonly carried out by reacting the free amino group at the C2 position or the hydroxyl groups at the C3 and C6 positions, leading to chitosan derivatives with enhanced solubility, mechanical stability, and functional performance [10].

One effective modification approach is cross-linking, in which chitosan chains are interconnected through covalent or non-covalent bonds using suitable cross-linking agents [11]. Cross-linked chitosan derivatives generally exhibit improved thermal stability, mechanical strength, and resistance to acidic conditions compared to native chitosan. Furthermore, cross-linking often enhances the hydrophilicity and swelling behavior of chitosan-based materials, which are critical parameters for biomedical and antibacterial applications. Previous studies have demonstrated that chitosan hydrogels cross-linked with various agents exhibit increased water absorption and enhanced antibacterial activity due to higher positive charge density and improved interaction with bacterial cell membranes [12, 13].

Polyethylene glycol (PEG) is a hydrophilic, biocompatible, non-toxic polymer that is widely used in biomedical applications. PEG possesses a high hydration capacity and chemical stability, making it an attractive cross-linking agent for improving the hydrophilicity and swelling behavior of polymeric materials [5]. In many chitosan-based systems, low-molecular-weight PEG, such as PEG-400 (a diol), is typically incorporated as a hydrophilic modifier or blending component, where it mainly interacts with the polymer matrix. Several studies have reported that PEG-modified chitosan systems exhibit enhanced water uptake, improved flexibility, and favorable antibacterial properties [14, 15]. The incorporation of PEG into chitosan networks has also been shown to increase solubility and swelling behavior without significantly compromising antibacterial performance.

In addition to cross-linking, the formation of Schiff bases via the reaction of chitosan amine groups with aldehydes is another effective strategy for chitosan modification. Schiff base formation introduces imine (C=N) functional groups that can enhance antibacterial activity through stronger interactions with bacterial cell components. Salicylaldehyde is an aromatic aldehyde containing a hydroxyl group that can form intramolecular hydrogen bonds with the imine nitrogen, contributing to increased structural stability of the resulting Schiff base. Imine (C=N) bonds are generally reversible and may undergo hydrolysis under acidic aqueous conditions. Protonation of the imine nitrogen can facilitate nucleophilic attack by water, thereby partially regenerating the corresponding amine and aldehyde.

Despite this intrinsic reversibility, the stability of aromatic Schiff bases is typically higher than that of aliphatic analogs due to conjugation with the aromatic ring and possible intramolecular hydrogen bonding. In the case of salicylaldehyde-derived Schiff bases, the presence of an ortho-hydroxyl group can provide additional stabilization through hydrogen bonding interactions. Moreover, under mildly acidic conditions, such as dilute acetic acid, and in near-neutral environments relevant to biomedical applications, the imine functionality is expected to remain sufficiently stable while retaining dynamic character. This balance between stability and reversibility may be advantageous for materials intended for moist environments, such as wound dressings or hydrogel-based systems [16].

Based on these considerations, the present study focuses on the synthesis of a Salicylaldehyde–chitosan Schiff base, followed by modification with polyethylene glycol. The formation of Schiff base is expected to enhance antibacterial activity through the introduction of imine functional groups, while PEG is anticipated to improve hydrophilicity and swelling behavior. The resulting PEG-modified Salicylaldehyde–chitosan Schiff base is expected to exhibit improved physicochemical properties while maintaining effective antibacterial activity, making it a promising material for potential biomedical and antimicrobial applications.

2. Experimental

2.1. Materials and Tools

The materials needed during this research were industrial chitosan (MW of 147,926.23 g/mol; degree of deacetylation of 67%), salicylaldehyde (Merck), glacial acetic acid (analytical grade) (Merck), NaCl, distilled water, 70% ethanol, NaOH, polyethylene glycol-400 (average MW ≈ 400 g mol^{-1}; density ≈ 1.13 g mL^{-1} at 25°C), Whatman filter paper, aluminum foil, universal pH indicator, yeast (Merck), peptone (Merck), nutrient agar (Merck), stock cultures of *Escherichia coli* obtained from the Biotechnology Laboratory, Department of Biology, FSM Undip, ciprofloxacin (Hexpharm Jaya).

The tools used during the study were analytical balance (Ohaus Pioneer P214), Ubbelohde viscometer, research standard glassware, a set of reflux apparatus, hot plate and magnetic stirrer (Vision VS-130SH),

magnetic bar, vacuum pump (Value), oven (Binder), desiccator, autoclave, Lamin Air Flow (Innotech), loop needle, bunsen, petri dish, spreader, 10-100 L micropipette (Thermo), tip, tweezers, ruler, incubator (Memert IN55), Orbital shaker (TS- 330A), UV-Vis (Ultraviolet-Visible) spectrophotometer (Genesys 10S), Frontier Fourier Transform Infrared (FTIR) spectrophotometer (Perkin Elmer 96681).

2.2. Experimental Procedures

2.2.1. Determination of Chitosan Molecular Weight

Preparation of 1% (w/v) chitosan solution was carried out by dissolving 1 g of chitosan in 25 mL of 1% acetic acid solvent and 75 mL of 0.2 M NaCl. The solution was stirred using a stirrer until homogeneous to maximize the dissolution of macromolecules from chitosan. The solution was then diluted to several concentrations: 0.1, 0.2, 0.3, 0.4, and 0.5%. Viscosity was measured using the method of Czechowska-Biskup *et al.* [17] using the Ubbelohde capillary viscometer. A total of 10 mL of solvent was placed into the Ubbelohde viscometer. The solvent flow time was measured 5 times. After rinsing and drying the capillaries, the flow time of the chitosan solution was measured for a series of concentrations. The flow time measurement was repeated for each concentration variation, and each concentration was measured 5 times. The flow time data obtained were used to calculate the specific viscosity, defined as the ratio of the change in flow time due to the addition of solute (t) to the flow time of the pure solvent (t_0). The specific viscosity (η_{sp}) and reduced viscosity (η_{red}) values are denoted in Equations 1 and 2, respectively.

$$\eta_{sp} = \frac{t-t_0}{t_0} \quad (1)$$

$$\eta_{red} = \frac{\eta_{sp}}{C} \quad (2)$$

The specific viscosity is used to calculate the reduced viscosity, which is the ratio of specific viscosity to solute concentration. The reduced viscosity data for each concentration were then converted to a graphical form to obtain the intrinsic viscosity. The intrinsic viscosity $[\eta]$ depends on the specific volume of the polymer, which is related to its molecular weight, and the solvent interactions of the polymer. The relationship between the intrinsic viscosity $[\eta]$ and the average molecular weight of the viscosity, i.e., M_v, is expressed by the following Mark-Houwink equation, shown in Equation 3.

$$[\eta] = KM_v^{\alpha} \quad (3)$$

K and α are constant characteristics for a given polymer-solvent system at a given temperature, and $[\eta]$ is the intrinsic viscosity of the polymer in the solution. Constants K and α also depend on the degree of deacetylation of chitosan and apply to a certain range of molecular weights.

2.2.2. Determination of the Degree of Deacetylation of Chitosan

The degree of deacetylation of chitosan was determined using Fourier Transform Infrared (FTIR) spectroscopy in the wavenumber range of 4000–400 cm^{-1}. The degree of deacetylation value was calculated using the baseline method, which is based on the ratio of the absorbance of the amide I band to that of the hydroxyl band. In this method, the amide I band at approximately 1655 cm^{-1} (A_{1655}), corresponding to the C=O stretching vibration of the N-acetyl group, and the hydroxyl stretching band at approximately 3450 cm^{-1} (A_{3450}) were selected as reference peaks. Before calculation, baseline correction was applied to the FTIR spectra to determine absorbance values at the selected wavenumbers. The absorbance values obtained from FTIR spectra are dimensionless quantities, and the ratio of these absorbances is used to estimate the degree of acetylation remaining in the chitosan structure. The degree of deacetylation is obtained using Equation 4.

$$\%DD = 100 - [\left(\frac{A_{1655}}{A_{3450}}\right) \times \frac{100}{1.33}] \quad (4)$$

Where, A_{1655} is the absorbance at the wavenumber ~1655 cm^{-1}, which is the absorption of the carbonyl group of the amide, A_{3450} is the absorbance at wave number ~3450 cm^{-1}, which is the absorption of the hydroxyl group (-OH), and 1.33 is the constant obtained from the ratio of A_{1655} to A_{3450} for un-deacetylated chitin [18].

2.2.3. Synthesis of Salicylaldehyde-Chitosan Schiff Base

A total of 1 g (6.172 mmol) of chitosan was dissolved in 50 mL of 3% (v/v) acetic acid, and then 50 mL of 70% ethanol was added. After that, salicylaldehyde was added slowly in three mole amounts: 4.5064 mmol (0.47 mL), 4.853 mmol (0.51 mL), and 5.1997 mmol (0.54 mL). The reaction was carried out by stirring with a stirrer in a reflux device at 60°C for 3 hours. The product was precipitated with 5% NaOH, yielding a yellow precipitate. Then the precipitate was filtered using a Buchner funnel and rinsed using distilled water periodically until the pH was neutral, followed by washing with 30 mL of 70% ethanol. The product was dried in an oven for 5 hours until a constant mass was obtained at a temperature of 70°C [19]. The synthesis results were analyzed using a UV-Vis spectrophotometer, and the degree of substitution was determined by FTIR spectroscopy [20, 21]. The synthesis was scaled up using 20 g (0.123 mol) of chitosan, which was reacted with 9.44 mL (0.09 mol) of salicylaldehyde.

2.2.4. Determination of the Degree of Substitution

The degree of substitution (DS) was calculated based on the deconvolution of the FTIR spectra in the wavenumber region of 1500–1800 cm^{-1}, where the characteristic absorption bands of the imine group (C=N), carbonyl group (C=O), and aromatic C=C appear. The degree of substitution was estimated by comparing the integrated area of the imine peak with the total area of the relevant peaks in this region, as defined in Equation 5.

$$Degree\ of\ Substitution\ (\%) = \frac{A_{C=N}}{A_{C=N} + A_{C=O} + A_{C=C}} \times 100 \quad (5)$$

Where, $A_{C=N}$ represents the integrated area of the imine absorption band, while $A_{C=O}$ and $A_{C=C}$ correspond to the integrated areas of the carbonyl and aromatic bands obtained from the deconvoluted FTIR spectra [22].

2.2.5. Preparation of Polyethylene Glycol-modified Salicylaldehyde-Chitosan Schiff Base

A total of 2 g (4.35 mmol) of salicylaldehyde-chitosan Schiff base was dissolved in 80 mL of 3% (v/v) acetic acid to form a brownish homogeneous solution. Then 2.048 mL or 5.78 mmol of polyethylene glycol-400 (PEG-400) was slowly added to the solution, which was stirred for 24 hours at 27°C. The precipitation process was carried out by adding 220 mL of 5% (w/v) NaOH until a yellow solid was formed. The precipitate was then separated from the filtrate using a Buchner funnel and rinsed with distilled water to obtain a neutral-pH precipitate. Rinsing continued with 30 ml of ethanol. The precipitate was successfully filtered and then dried in an oven at 70°C for approximately 3 hours to obtain a constant mass. The synthesis results were analyzed by the FTIR spectrophotometer and the UV-Vis spectrophotometer [15, 23].

2.2.6. Swelling Percentage Measurement

The swelling percentage was determined by comparing the dry mass and the wet mass of the sample. The samples tested included chitosan, salicylaldehyde-chitosan Schiff base, and PEG-modified salicylaldehyde-chitosan Schiff base. Each sample of 100 mg was immersed in a vial containing 2 mL of distilled water for 24 hours at room temperature. Then the samples were separated using filter paper and weighed again [24]. The percentage of swelling is calculated using Equation 6.

$$\%Swelling = \frac{W_w - W_d}{W_d} \times 100\% \quad (6)$$

Where, W_w is the wet weight of the sample after immersion and W_d is the weight of the dry sample [5].

2.2.7. Contact Angle Measurement

The contact angle was determined using the sessile drop method. The samples tested were chitosan, salicylaldehyde-chitosan Schiff base, and PEG-modified salicylaldehyde-chitosan Schiff base with a concentration of 2500 ppm each in 10 mL of 3% acetic acid. Membranes were prepared by casting the solution into a petri dish and drying at 100 °C for ~30 minutes. The dried membrane was soaked in 5% NaOH until detached, rinsed to neutral, and air-dried [25]. The contact angle was measured using the sessile drop method. The contact angle was measured using the sessile drop method. A small droplet of distilled water (~5 µL) was carefully deposited on the membrane surface (approximately 1 × 1 cm^2) placed on a level substrate to minimize measurement error. Droplet images were captured using a Samsung M31 macro camera under controlled lighting. Contact angles were analyzed with ImageJ (LB-ADSA plugin). It should be noted that simple spherical fitting methods may introduce some limitations; therefore, this approach was used primarily for comparative screening of surface wettability rather than precise surface energy determination [26].

2.2.8. Antibacterial Test

The antibacterial activity of chitosan, Salicylaldehyde–chitosan Schiff base, and PEG-modified Salicylaldehyde–chitosan Schiff base was evaluated using the disc diffusion method against *Escherichia coli* (Gram-negative) and *Staphylococcus aureus* (Gram-positive). Ciprofloxacin (0.03 mg/mL) and 2% (v/v) acetic acid were used as positive and negative controls, respectively. Bacterial suspensions were prepared and standardized to the McFarland 0.5 turbidity (≈10^8 CFU/mL). Test samples were prepared at a concentration of 1 mg/mL in 2% (v/v) acetic acid. Aliquots of the bacterial suspensions (40 µL) were spread onto nutrient agar plates, and sterile paper discs (0.5 cm diameter) impregnated with 10 µL of each test solution were placed on the agar surface. The plates were incubated at 37°C, and antibacterial activity was assessed by measuring the inhibition zone diameters at 8, 12, 16, and 24 hours.

3. Results and Discussion

3.1. Characteristics of Chitosan

The characteristics of chitosan, including molecular weight and degree of deacetylation, were determined because these parameters strongly influence its physicochemical properties and suitability for further chemical modification and antibacterial applications [17]. The molecular weight of chitosan was determined by viscometry using a Ubbelohde viscometer. Chitosan solutions with concentrations of 0.001–0.005 g mL^{-1} were prepared using a mixed solvent of 1% (v/v) acetic acid and NaCl (3:1). Chitosan dissolves in dilute acidic media due to the protonation of its amino groups, which increases its solubility in aqueous solution. The addition of NaCl serves to control the ionic strength of the solution and to screen electrostatic repulsion between the protonated chitosan chains. This ionic shielding helps minimize intermolecular electrostatic interactions, enabling more reliable viscosity measurements during molecular weight determination. The protonation of the amine groups of chitosan results in the formation of protonated chitosan salts, as illustrated in Figure 1.

The results of measuring the flow time of the chitosan solution at concentrations of 0.001, 0.002, 0.003, 0.004, and 0.005 g/mL are shown in the graph of η_{red} vs. concentration (Figure 2). In Figure 2, it is concluded that it is proportional to the reduced viscosity. The regression equation obtained from the plot of reduced viscosity (η_{red}) versus concentration is y = 12.639x + 1.1765. The intercept corresponds to the intrinsic viscosity [η] = 1.1765 dL g^{-1}. The molecular weight of chitosan was calculated using the Mark–Houwink equation $[\eta] = KM^a$, using literature constants for chitosan in acidic salt solution (K ≈ 1–2 × 10^{-3} dL g^{-1}, a ≈ 0.8–0.9) at room temperature. The molecular weight of chitosan is 147926.23 g/mol with a total of 913 monomers.

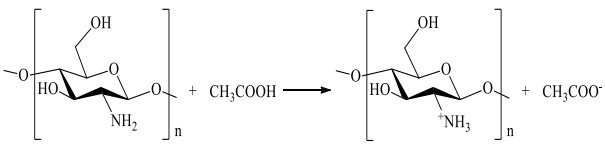

Figure 1. The protonation reaction of the amine group of chitosan in acetic acid solvent

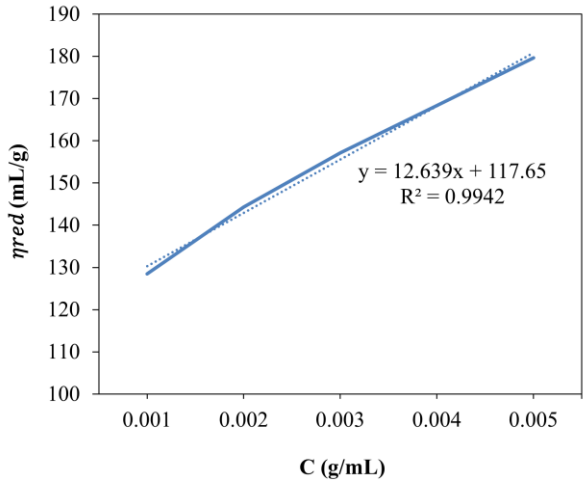

Figure 2. Graph of the relationship between concentration and viscosity reduction

FTIR spectrophotometry is one of the methods used to analyze functional groups in a compound. To determine the degree of deacetylation, infrared spectrophotometric analysis was performed using the baseline method in the functional group and fingerprint regions, with a wavenumber range of 4000 cm^{-1} to 400 cm^{-1}. Based on the calculations, the degree of deacetylation is 67%, indicating that 612 chitosan monomers have free amine groups out of a total of 913. Theoretically, chitosan has an amide group of 33%. The infrared spectra of chitosan are presented in Figure 3. The infrared spectrum of chitosan showed an absorption at 3370.45 cm^{-1}, indicating stretching vibrations of the hydroxyl (−OH) and amine ($-NH_2$) groups, which overlapped, broadening the absorption peak. The −NH group observed comes from the free amine and the secondary amide that is not deacetylated. The absorption of the $-NH_2$ group is smaller than the absorption of the –OH group because the bonds tend to be weaker. Absorption also appears at 1652.00 cm^{-1}, indicating a strain vibration of the carboxyl group (C=O) of the undeacetylated acetyl group of chitosan. The interpretation of chitosan infrared absorption data is shown in Table 1.

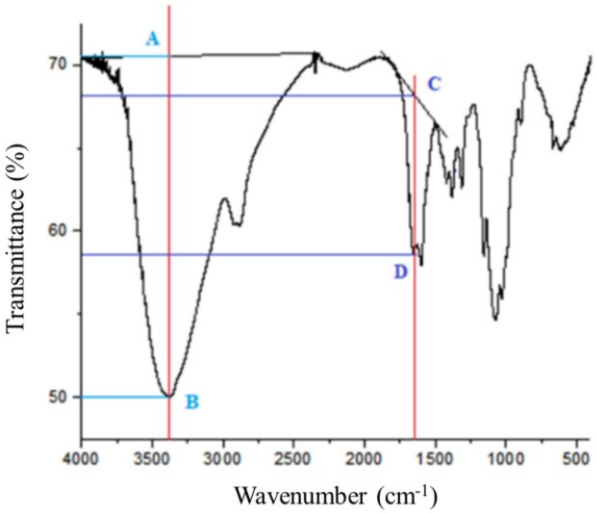

Figure 3. Infrared spectrum of chitosan

Table 1. Data interpretation of the absorption of the functional group of chitosan compounds on infrared spectrophotometry

Wavenumber (cm^{-1})	Functional group vibration
3370.45	Stretching O−H and N−H
2881.5	Stretching >CH− aliphatic
1652	Stretching C=O
1597.04	Bending >N-H
1380.05	Bending >CH− aliphatic
1072.78	Stretching C-O-C

3.2. Synthesis and Characteristics of Salicylaldehyde-Chitosan Schiff Base

Synthesis of salicylaldehyde-chitosan Schiff base was carried out for synthesis by forming an imine group. The synthesis process involves nucleophilic addition and dehydration reactions. The reaction occurs when the nitrogen atom of the amine in chitosan, acting as a nucleophile, attacks the carbon atom of the aldehyde group in salicylaldehyde, forming an imine. Chitosan and salicylaldehyde were dissolved in 3% (v/v) acetic acid and 70% ethanol, respectively. The reaction that occurs can be proposed as shown in Figure 4 [27].

Figure 4 shows that the formation of a Schiff base or imine group (C=N) occurs along with the introduction of a hydroxy-substituted benzene ring (−OH). The presence of a hydroxy group near the imine functionality allows intramolecular hydrogen bonding between the nitrogen atom of the imine and the phenolic hydroxyl hydrogen. These hydrogen-bonding interactions contribute to increasing the structural stability of the Salicylaldehyde–chitosan Schiff base. It should be noted that imine bonds are generally reversible and may undergo hydrolysis in acidic aqueous environments, where protonation of the imine nitrogen can facilitate nucleophilic attack by water and lead to regeneration of the corresponding amine and aldehyde. However, in the present system, the imine group is conjugated with the aromatic ring of salicylaldehyde and further stabilized by intramolecular hydrogen bonding involving the ortho-hydroxyl group. These stabilizing effects can reduce the susceptibility of the C=N bond to rapid hydrolysis compared with non-aromatic imines. Therefore, under the relatively mild acidic conditions used in this study, the Salicylaldehyde–chitosan Schiff base is expected to maintain sufficient structural stability while still exhibiting the dynamic character typical of Schiff base linkages.

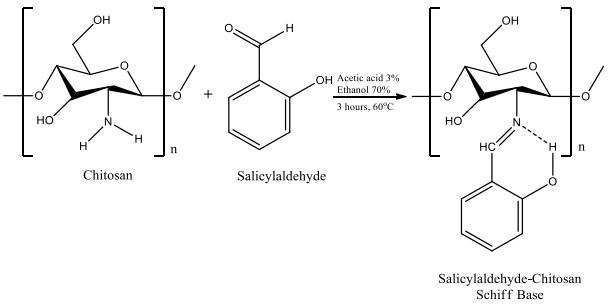

Figure 4. General reaction of salicylaldehyde-chitosan Schiff base synthesis

Table 2. Mass of the synthesized Salicylaldehyde–chitosan Schiff (CS) product

No.	Chitosan Mass (g)	Salicylaldehyde Mass (g)	Product Name	Theoretical Mass (g)	Product Mass (g)	Yield (%)
1	1.000	0.550	CS-667	1.469	0.58	39.49
2	1.000	0.593	CS-718	1.506	0.48	31.87
3	1.000	0.635	CS-769	1.543	0.55	35.63

The product was obtained as a brownish-yellow solid. The salicylaldehyde–chitosan Schiff base was synthesized using three molar variations of salicylaldehyde, theoretically corresponding to the formation of 667, 718, and 769 imine groups on the chitosan backbone. However, based on the synthesis yield, the number of imine groups formed did not reach these theoretical values, indicating that the degree of substitution did not achieve 100%. The mass of the products obtained from the three salicylaldehyde molar variations is presented in Table 2.

The highest yield was obtained for the system corresponding to 667 monomers. Increasing the amount of salicylaldehyde initially enhanced the yield; however, further addition led to a decrease in the amount of salicylaldehyde–chitosan Schiff base produced. At higher concentrations, the available reactive space becomes more restricted, limiting effective molecular interactions and hindering the reaction. This suggests that while increasing reactant concentration can improve yield, an excess beyond the optimal level may inhibit the reaction [28].

3.2.1. Analysis of Salicylaldehyde-Chitosan Schiff Base Using FTIR

An infrared spectrophotometer was used to analyze the functional groups in the synthesized product. This analysis aimed to confirm the success of the substitution reaction, as indicated by the conversion of the amine group ($-NH_2$) in chitosan to an imine (C=N) group characteristic of a Schiff base. The reduction or disappearance of N–H absorption, both in stretching and bending vibrations, supports this transformation. However, the N–H stretching vibration in the ~3400 cm^{-1} region overlaps with the O–H stretching band, making it difficult to clearly observe its reduction. Therefore, the analysis was focused on the 1550–1700 cm^{-1} region, where the appearance of the C=N stretching vibration and the decrease in N–H bending vibration can be more clearly identified. The FTIR spectra of chitosan and the salicylaldehyde–chitosan Schiff base with three variations are presented in Figure 5.

Based on the spectra shown in Figure 5, native chitosan exhibited an absorption band at 1652 cm^{-1} corresponding to the stretching vibration of the carbonyl group (C=O) from the residual acetyl groups (Amide I band). After the reaction with salicylaldehyde, the spectra of the Salicylaldehyde–chitosan Schiff base showed a shift of this absorption band to lower wavenumbers at 1639.08, 1648.49, and 1640.75 cm^{-1}. This shift in peak position is an important indication of the formation of the imine (C=N) group resulting from the reaction between the amine group of chitosan and the aldehyde group of salicylaldehyde. In addition, no distinct absorption band was observed around ~1700 cm^{-1}, which would correspond to the carbonyl stretching vibration of unreacted aldehyde groups, indicating that the remaining salicylaldehyde impurity after purification was minimal. Furthermore, the reduced intensity of the N–H bending vibration around ~1597 cm^{-1} supports the consumption of amine groups during the formation of the Schiff base. These spectral changes—including the shift in the 1600–1650 cm^{-1} region and the decrease in N–H bending absorption—collectively support the successful conversion of chitosan amine groups into imine (C=N) functionalities.

The infrared spectra were also used to determine the degree of substitution. By evaluating the degree of substitution of each sample, the extent of imine group formation relative to the original amine groups can be assessed, allowing identification of the optimal salicylaldehyde molar variation. The degree of substitution was determined by deconvoluting the IR spectra of each product in the 1800–1500 cm^{-1} region to obtain the peak areas corresponding to the imine (C=N), carbonyl (C=O), and aromatic C=C groups. The degree of substitution was then calculated by comparing the area of the imine peak to the total area of these three bands. The deconvoluted spectra are presented in Figure 6, while the corresponding peak areas and calculated degree of substitution values for the three salicylaldehyde–chitosan Schiff base samples are summarized in Table 3.

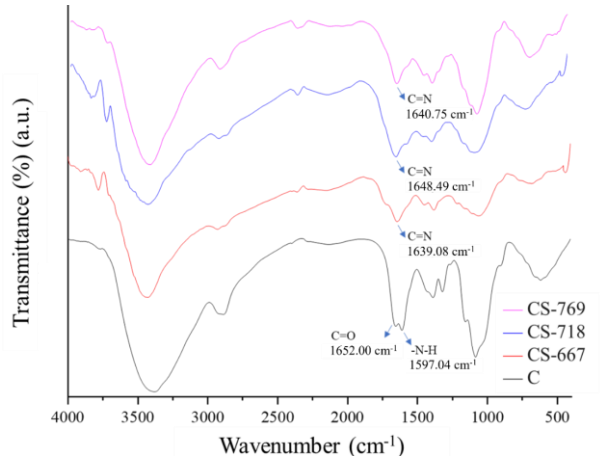

Figure 5. Infrared spectra of chitosan (C) and salicylaldehyde-chitosan Schiff base (CS) with three-mole variations of salicylaldehyde

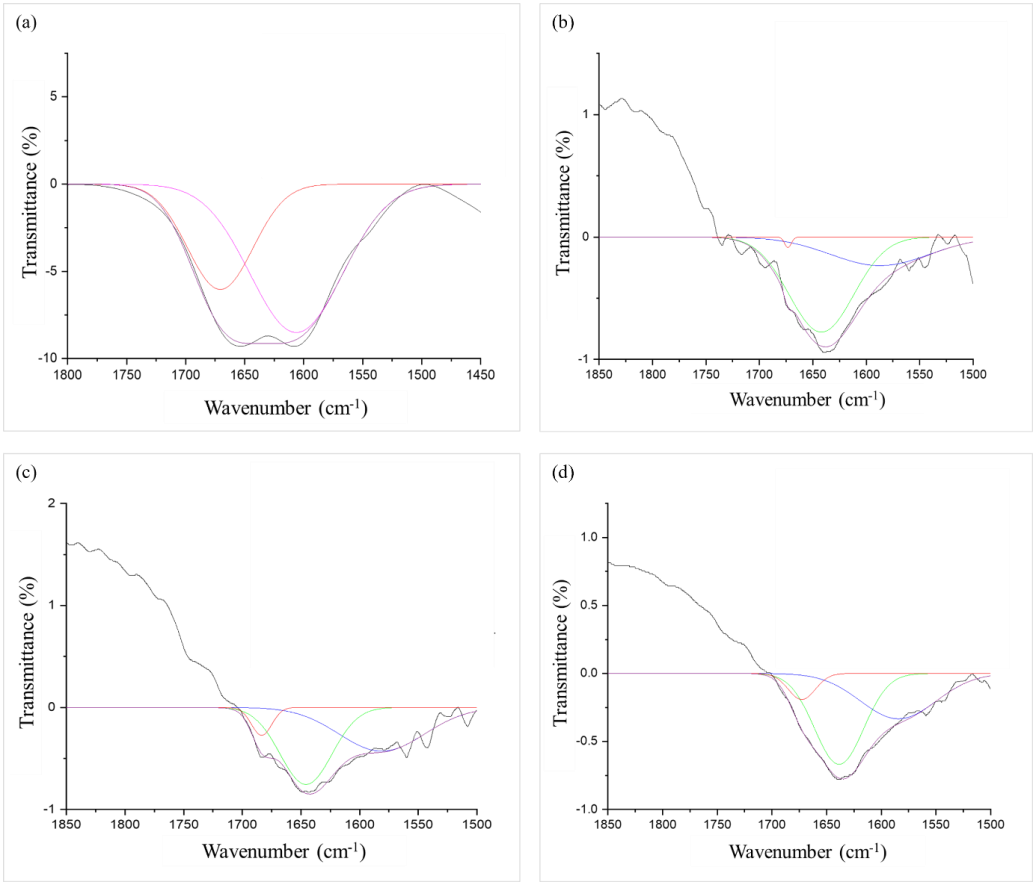

Figure 6. Deconvolution of IR spectra (a) chitosan (C), salicylaldehyde-chitosan Schiff base (CS) variations of (b) 667 monomers, (c) 718 monomers, and (d) 769 monomers

Table 3. Substitution data for salicylaldehyde-chitosan Schiff base (CS)

No.	Compound	Area			Degree of Substitution (%)
		C=C	C=N	C=O	
1	C	-	-	33.46	0
2	CS-667	30.64	68.57	0.79	68.57
3	CS-718	44.73	48.39	6.88	48.38
4	CS-769	39.76	52.00	8.23	52

Based on Table 3, the highest degree of substitution was obtained for the variation corresponding to 667 monomers of salicylaldehyde. This is consistent with the yield results, indicating that increasing the amount of salicylaldehyde reduces the effective reaction space [28]. Consequently, molecular interactions become more limited, leading to the formation of fewer imine groups and a lower degree of substitution.

3.2.2. Analysis of Salicylaldehyde-Chitosan Schiff Base Using UV-Vis Spectrophotometry

The synthesized salicylaldehyde–chitosan Schiff base was further analyzed using UV–Vis spectroscopy to confirm the conversion of amine groups into imine groups. The UV–Vis spectra of chitosan and the salicylaldehyde–chitosan Schiff base are presented in Figure 7.

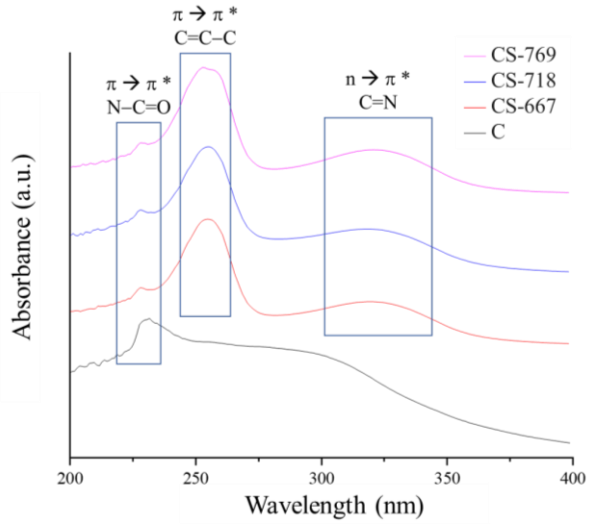

Figure 7. Comparison of UV-Vis spectra of chitosan (C) and salicylaldehyde-chitosan Schiff base (CS)

Table 4. UV absorption data for chitosan (C) and salicylaldehyde-chitosan Schiff base (CS) compounds

Sample	Variation of Salicylaldehyde (g)	Wavelength (nm)		
		Band I	Band II	Band III
C	-	232	273	-
CS-667	0.550	236	255	321
CS-718	0.593	233	255	320
CS-769	0.635	238	255	321

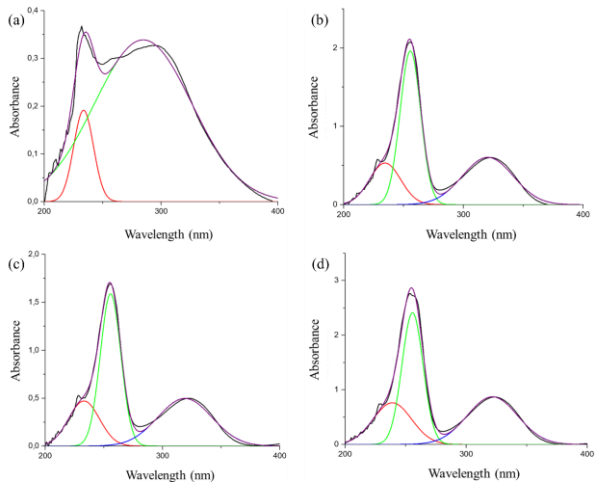

Figure 8. Deconvolution of UV-Vis spectra: (a) chitosan (C), salicylaldehyde-chitosan Schiff base (CS) variations of (b) 667 monomers, (c) 718 monomers, and (d) 769 monomers

The chitosan used was not fully deacetylated; therefore, residual amide carbonyl groups from chitin remain. This is evident from the deconvoluted spectrum of chitosan, which shows two absorption bands at 232 nm (band I), corresponding to the π → π* transition of the amide system, and at 273 nm (band II), assigned to the n → π* transition. In salicylaldehyde-chitosan Schiff bases (three molar variations), band I appears at 236, 233, and 238 nm (π → π* of the amide system). Band II is observed at 255, 255, and 253 nm, respectively, and is attributed to the π → π* transition of the C=N group and the conjugated benzene ring substituted with an OH group. Additionally, all three samples exhibit a third absorption band (band III) at 321, 320, and 321 nm, respectively, which corresponds to the n → π* transition of the imine group and the conjugated benzene ring with hydroxyl substitution. The absorption data of the salicylaldehyde–chitosan Schiff base are summarized in Table 4, while the deconvoluted UV–Vis spectra are presented in Figure 8.

From Figure 7, it can be concluded that imine groups were successfully formed in all variations of the salicylaldehyde–chitosan Schiff base, as indicated by the absorption band around 320 nm. This band corresponds to the n → π* electronic transition of the imine group conjugated with a hydroxyl-substituted benzene ring. However, the UV–Vis spectra cannot be used to quantify the degree of substitution; therefore, the extent of the reaction cannot be determined quantitatively based on UV–Vis data alone.

3.3. Synthesis and Characteristics of PEG-modified Salicylaldehyde-Chitosan Schiff Base

Polyethylene glycol-modified Schiff salicylaldehyde-chitosan was synthesized by reacting 2 g (4.35 mmol) of Schiff salicylaldehyde-chitosan base with 2 mL (5.78 mmol) polyethylene glycol (PEG). The PEG-modified salicylaldehyde-chitosan Schiff base synthesis yielded a brown product (1.515 g) with a 40.49% yield. The solvent used to dissolve chitosan and PEG was 3% acetic acid. Based on the spectroscopic data, the reaction that occurs can be proposed in Figure 9 [15].

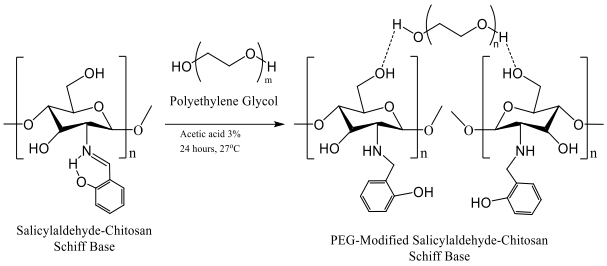

Figure 9. General reaction of salicylaldehyde-chitosan Schiff base with PEG

The reaction occurs between the hydroxyl group of PEG and the carbon of the imine group (–C=N). The hydroxyl group, which acts as a nucleophile, attacks the carbon of the imine group, which is partially positively charged, so that an addition reaction occurs. PEG has two hydroxyl groups (–OH) at both ends. The two hydroxyl groups separately react with two different Schiff bases of chitosan.

3.3.1. Analysis of PEG-modified Salicylaldehyde-Chitosan Schiff Base Using FTIR

PEG-modified salicylaldehyde-chitosan Schiff base was analyzed using FTIR spectrophotometry. The analysis aims to determine the change of the imine group (C=N) or Schiff base into an amine group. The results of the FTIR spectrophotometric analysis of salicylaldehyde-chitosan Schiff base and PEG-modified salicylaldehyde-chitosan Schiff base can be seen in Figure 10.

The infrared spectra of the salicylaldehyde-chitosan Schiff base showed absorption at a wavenumber of 1647.75 cm^{-1}, which was the stretch vibration absorption of the imine group (C=N), while in the PEG-modified salicylaldehyde-chitosan Schiff base, the absorption occurred at a wavenumber of 1557.75 cm^{-1}, indicating a bending vibration of the >N–H group. This indicates that the imine group on the salicylaldehyde-chitosan Schiff base has changed and no longer appears in the PEG-modified salicylaldehyde-chitosan Schiff base spectra. Infrared spectrophotometric interpretation data can be shown in Table 5.

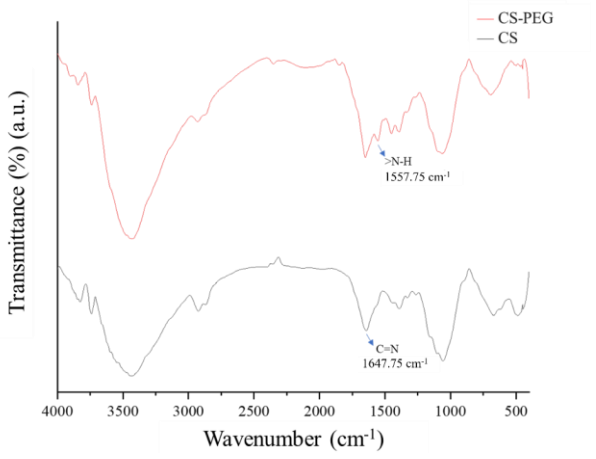

Figure 10. Infrared spectra of salicylaldehyde-chitosan Schiff base (CS) and PEG-modified salicylaldehyde-chitosan Schiff base (CS-PEG)

Table 5. Interpretation of functional group absorption data from salicylaldehyde-chitosan Schiff base (CS) and PEG-modified salicylaldehyde-chitosan Schiff base compound (CS-PEG)

No.	Wavenumber (cm^{-1})		Functional group vibration
	CS	CS-PEG	
1	3442.5	3431.00	Stretching O–H and N–H
2	2925.5	2927.75	Stretching >CH– aliphatic
3	-	1661.00	Stretching C=O
4	1647.75	-	Stretching C=N
5	-	1557.75	Bending >N–H
6	1454.75	1456.25	Bending >C–H_2
7	1381.75	1385.25	Bending >C–H– aliphatic
8	1157.00	1155.50	Stretching C–O–C

The appearance of an absorption peak in the ~1557 cm^{-1} region in the infrared spectra of the PEG-modified salicylaldehyde-chitosan Schiff base. indicated the presence of >N–H bending vibrations, which the salicylaldehyde-chitosan Schiff base did not have. This indicates that the imine group is absent and that bonding to PEG has been successful.

3.3.2. Analysis of PEG-modified Salicylaldehyde-Chitosan Schiff Base Using UV-Vis Spectrophotometry

The synthesized PEG-modified salicylaldehyde-chitosan Schiff base was analyzed using a UV-Vis spectrophotometer to confirm that the imine group in the salicylaldehyde-chitosan Schiff base had turned into an amine group. The UV-Vis spectra of the two compounds are presented in Figure 11. Based on Figure 11, an absorption band (band I) at 245 nm corresponds to the $\pi \rightarrow \pi^*$ transition of the amide system. Band II, observed at 256 nm, is attributed to the $\pi \rightarrow \pi^*$ transition of the imine group (C=N) and the conjugated benzene ring substituted with a hydroxyl group (–OH). In addition, a third absorption band (band III) appears at 314 nm, corresponding to the $n \rightarrow \pi^*$ transition of the imine group and the conjugated benzene ring with hydroxyl substitution.

For the PEG-modified salicylaldehyde - chitosan Schiff base, two main absorption bands are observed at 238 nm (band I), representing the $\pi \rightarrow \pi^*$ transition of the amide system, and at 279 nm (band II), corresponding to the $\pi \rightarrow \pi^*$ transition of the hydroxyl-substituted benzene ring. In both the unmodified and PEG-modified Schiff base samples, the presence of amide carbonyl absorption indicates that the chitosan backbone was not fully deacetylated.

The deconvoluted spectra are presented in Figure 12, while the corresponding absorption data for both the salicylaldehyde–chitosan Schiff base and its PEG-modified derivative are summarized in Table 6. Based on the absorption observed in the PEG-modified salicylaldehyde–chitosan Schiff base, it can be inferred that a structural modification has occurred after PEG incorporation. The disappearance of the absorption peak at approximately 314 nm, which corresponds to the $n \rightarrow \pi^*$ transition of the imine (C=N) group, indicates a change in the electronic environment of the imine functionality compared to the original Schiff base (CS). However, under the mild reaction conditions employed, this modification is more appropriately attributed to physical interactions, such as hydrogen bonding between PEG hydroxyl groups and functional groups in the Schiff base matrix, rather than to the formation of a covalent cross-linked network. Therefore, the spectral changes suggest PEG-induced modification of the polymer structure instead of definitive covalent crosslinking.

Table 6. UV absorption data for salicylaldehyde-chitosan Schiff base (CS) and PEG-modified salicylaldehyde-chitosan Schiff base (CS-PEG) compounds

Sample	Wavelength (nm)		
	Band I	Band II	Band III
CS	245	256	314
CS-PEG	238	279	-

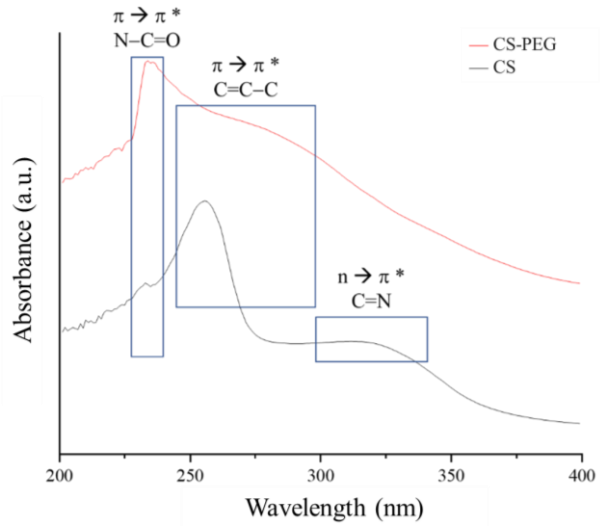

Figure 11. Comparison of spectra of salicylaldehyde-chitosan Schiff base (CS) and PEG-modified salicylaldehyde-chitosan Schiff base (CS-PEG)

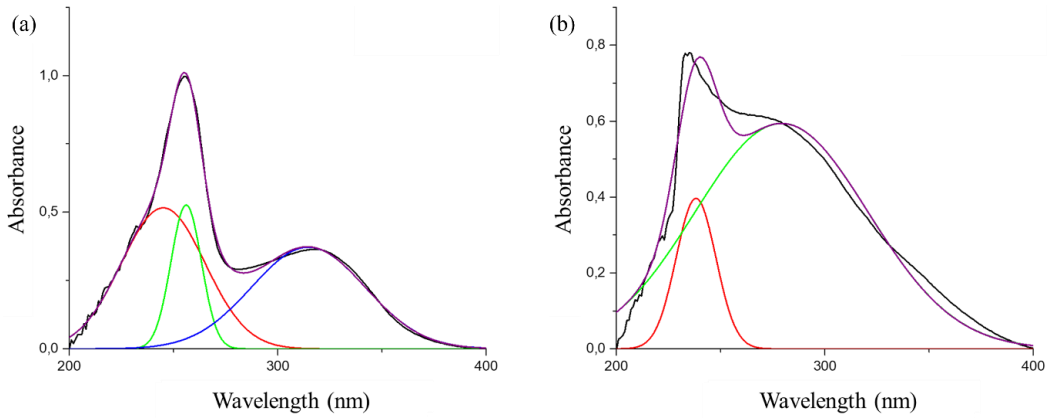

Figure 12. Deconvolution of UV-Vis spectra (a) salicylaldehyde-chitosan Schiff base (CS) and (b) PEG-modified salicylaldehyde-chitosan Schiff base (CS-PEG)

3.3.3. Physicochemical Properties of PEG-modified Salicylaldehyde-chitosan Schiff Base

The evaluated physical properties included swelling behavior and contact angle. The swelling degree is an important parameter for assessing the potential applications of chitosan and its derivatives. Swelling measurements were conducted in distilled water for 24 hours at room temperature. The contact angle was determined using the sessile drop method on membrane samples. The samples analyzed were chitosan, salicylaldehyde–chitosan Schiff base, and PEG-modified salicylaldehyde–chitosan Schiff base. The results of the swelling percentage and contact angle measurements for all samples are presented in Figure 13. Figure 13 shows that there was a decrease in the polarity of the Salicylaldehyde–chitosan Schiff base, which was indicated by an increase in the contact angle compared with native chitosan. This suggests that the Salicylaldehyde–chitosan Schiff base exhibits a relatively more hydrophobic surface than chitosan. In contrast, the PEG-modified salicylaldehyde–chitosan Schiff base exhibited the lowest contact angle, indicating increased surface hydrophilicity after PEG incorporation.

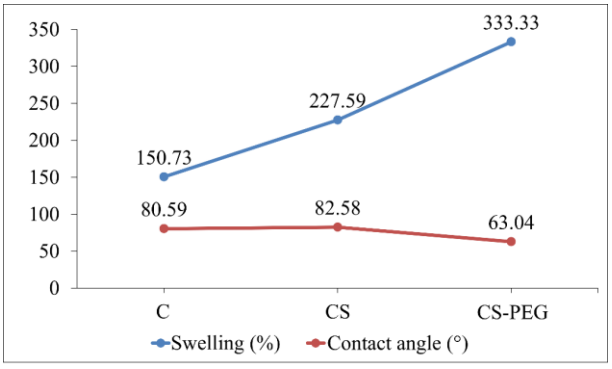

Figure 13. Graph of swelling percentage and contact angle of chitosan (C), salicylaldehyde-chitosan Schiff base (CS), and PEG-modified salicylaldehyde-chitosan Schiff base (CS-PEG)

The enhanced hydrophilicity of the PEG-modified material can be attributed to the intrinsic hydrophilic nature of PEG, which contains multiple ether (– C– O– C–) and hydroxyl groups capable of forming hydrogen bonds with water molecules. When PEG is incorporated into the chitosan/Schiff base matrix, it can interact with the polymer chains through hydrogen bonding and physical association, rather than forming covalent crosslinks. These interactions reduce the extent of interchain hydrogen bonding between chitosan chains and increase the free volume within the polymer matrix. As a result, water molecules can more easily penetrate the structure, leading to lower contact angles and greater swelling. Therefore, the improved wettability of the PEG-modified Salicylaldehyde–chitosan Schiff base is primarily attributed to PEG blending/association and its hydrophilic functional groups, which enhance water affinity and facilitate water uptake within the polymer network [29].

3.4. Antibacterial Activity Test

The antibacterial activity was evaluated using the disc diffusion method by measuring the inhibition zones against two bacterial strains, namely *Staphylococcus aureus* (Gram-positive) and *Escherichia coli* (Gram-negative). In this study, ciprofloxacin was used as a positive control due to its broad-spectrum antibacterial activity, acting through inhibition of bacterial DNA gyrase [30], while 2% acetic acid was used as a negative control because of its relatively weak antibacterial effect.

The test solutions consisted of chitosan, salicylaldehyde–chitosan Schiff base, and PEG-modified salicylaldehyde–chitosan Schiff base, each at a concentration of 1 mg/mL. The positive control (ciprofloxacin) was used at 0.03 mg/mL, while the negative control (2% acetic acid) was applied accordingly. The inhibition zones observed for all samples are presented in Table 7.

Table 7. Inhibitory zone data for chitosan (C), salicylaldehyde-chitosan Schiff base (CS), and PEG-modified salicylaldehyde-chitosan Schiff base (CS-PEG) compounds

No.	Sample	Concentration (mg/mL or mL/mL)	Inhibition zone (mm)			
			Escherichia coli		*Staphylococcus aureus*	
			8 hours	12 hours	8 hours	12 hours
1	Control +	0.03	15	13	18	16
2	Control -	2	8	9	9	8
3	C	1	9	8	10	9
4	CS	1	10	8	11	10
5	CS-PEG	1	9	8	10	9

Control (+) = ciprofloxacin (0.03 mg mL^{-1}); Control (−) = 2% (v/v) acetic acid. Bacterial suspensions were adjusted to a 0.5 McFarland standard. Inhibition zones were recorded at 8 and 12 h as part of an exploratory time-course measurement. These values are reported for comparative purposes and do not represent standardized susceptibility endpoints according to CLSI disc diffusion guidelines.

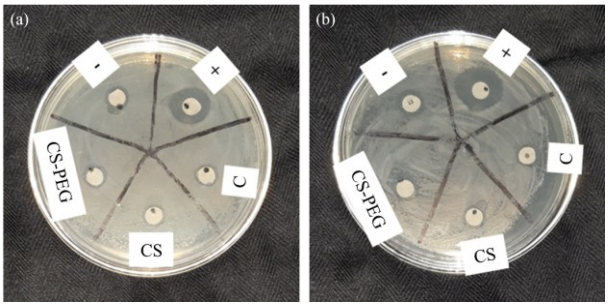

Figure 14. Antibacterial activity of chitosan, salicylaldehyde–chitosan Schiff base, and PEG-modified salicylaldehyde–chitosan Schiff base against (a) *Escherichia coli* and (b) *Staphylococcus aureus*

The inhibition zones decreased after 8 hours, indicating that the samples exhibit optimal antibacterial activity within the first 8 hours of application. The salicylaldehyde–chitosan Schiff base (CS) showed greater antibacterial activity than chitosan (C), as evidenced by its larger inhibition zones. This enhanced activity is attributed to the presence of the imine group, in which the nitrogen atom possesses a lone pair of electrons that can form hydrogen bonds with active sites on bacterial cells, thereby disrupting normal cellular processes.

In Gram-negative bacteria such as *Escherichia coli*, these interactions likely occur between the C=N group and the hydrophilic lipopolysaccharide layer. In contrast, for Gram-positive bacteria such as *Staphylococcus aureus*, hydrogen bonding occurs with the hydrophilic components of the peptidoglycan layer [31]. Additionally, the presence of –OH groups in the CS structure further contributes to the increased antibacterial activity [32].

The PEG-modified salicylaldehyde–chitosan Schiff base (CS-PEG) did not exhibit improved antibacterial activity compared to CS, likely because PEG crosslinking does not significantly contribute to antibacterial properties [14, 33, 34]. Overall, the salicylaldehyde–chitosan Schiff base demonstrated the highest antibacterial activity among the tested samples, with inhibition zone diameters of 10 mm against *Escherichia coli* and 11 mm against *Staphylococcus aureus*.

Antibacterial compounds are generally more effective against *Escherichia coli* than *Staphylococcus aureus* due to differences in their cell wall structures. Gram-negative bacteria, such as *Escherichia coli*, possess a thin peptidoglycan layer and an outer membrane composed of phospholipids and lipopolysaccharides, whereas Gram-positive bacteria, such as *Staphylococcus aureus*, lack an outer membrane but have a much thicker peptidoglycan layer [35, 36]. As a result, antibacterial agents are typically expected to exhibit greater activity against Gram-negative bacteria.

However, in this study, a larger inhibition zone was observed for *Staphylococcus aureus* compared to *Escherichia coli*. This deviation is likely due to differences in bacterial density, where the *Escherichia coli* suspension had a higher cell concentration than that of *Staphylococcus aureus*, thereby reducing the apparent inhibition zone. The inhibition zones observed against *Escherichia coli* and *Staphylococcus aureus* are presented in Figure 14.

4. Conclusion

Chitosan was successfully modified via Schiff base formation with salicylaldehyde, yielding a salicylaldehyde–chitosan Schiff base with a maximum degree of substitution of 68.75% and a yield of 41.08% (w/w) at 4.5064 mmol of salicylaldehyde. This indicates that the selected molar ratio was favorable for the formation of imine (C=N) groups along the chitosan backbone. Further modification through PEG incorporation produced a brown solid with a yield of 40.49% (w/w). Under the conditions employed, PEG incorporation is best described as physical blending rather than covalent crosslinking. The presence of PEG enhanced the hydrophilicity of the material, as reflected by an increased swelling ratio (333.33%) and a reduced contact angle (63.04°). These improvements are attributed to the hydrophilic nature of PEG and its ability to interact with the polymer matrix through hydrogen bonding and physical entanglement, thereby increasing water affinity and polymer chain mobility. Antibacterial activity showed inhibition zones of 9 mm against *Escherichia coli* and 10 mm against *Staphylococcus aureus*, comparable to those of the 2% acetic acid control, suggesting that the effect mainly arises from the acidic medium. Overall, the PEG-modified (PEG-blended) salicylaldehyde–chitosan Schiff base exhibits improved hydrophilicity and swelling behavior, indicating its potential for applications such as hydrophilic coatings, biomaterials, and polymer systems that require enhanced water affinity.

Acknowledgement

Thank you to the Faculty of Science and Mathematics, Diponegoro University (UNDIP), for supporting this publication through "Program Riset Madya 2021", Contract Number: 902/UN7.5.8.2/HK/2021.

References

[1] Karen C. Carroll, Jeffery A. Hobden, Steve Miller, Stephen A. Morse, Timothy A. Mietzner, Barbara Detrick, Thomas G. Mitchell, James H. McKerrow, Judy A. Sakanari, Chapter 9: Pathogenesis of Bacterial Infection, in: *Jawetz, Melnick, & Adelberg's Medical Microbiology*, McGraw-Hill Education, New York, NY, 2019,

[2] Wesley A. Volk, Margaret F. Wheeler, *Mikrobiologi Dasar*, 5 ed. ed., Erlangga, 1993,

[3] Daniela Campaniello, Maria Rosaria Corbo, Chitosan: a Polysaccharide with Antimicrobial Action, in: *Application of Alternative Food-Preservation Technologies to Enhance Food Safety and Stability*, Bentham Science, 2010, https://doi.org/10.2174/978160805096311001010092

[4] Anrong Zeng, Yangtao Wang, Dajun Li, Juedong Guo, Qiaowen Chen, Preparation and antibacterial properties of polycaprolactone/quaternized chitosan blends, *Chinese Journal of Chemical Engineering*, 32, (2021), 462-471 https://doi.org/10.1016/j.cjche.2020.10.001

[5] Arman Jafari, Shadi Hassanajili, Negar Azarpira, Mohammad Bagher Karimi, Bita Geramizadeh, Development of thermal-crosslinkable chitosan/maleic terminated polyethylene glycol hydrogels for full thickness wound healing: *In vitro* and *in vivo* evaluation, *European Polymer Journal*, 118, (2019), 113-127 https://doi.org/10.1016/j.eurpolymj.2019.05.046

[6] Ji-Ung Park, Eun-Ho Song, Seol-Ha Jeong, Juha Song, Hyoun-Ee Kim, Sukwha Kim, Chitosan-Based Dressing Materials for Problematic Wound Management, in: H.J. Chun, K. Park, C.H. Kim, G. Khang (Eds.) *Novel Biomaterials for Regenerative Medicine*, Springer Nature Singapore, Singapore, 2018, https://doi.org/10.1007/978-981-13-0947-2_28

[7] Yaowen Liu, Shuyao Wang, Wenting Lan, Fabrication of antibacterial chitosan-PVA blended film using electrospray technique for food packaging applications, *International Journal of Biological Macromolecules*, 107, (2018), 848-854 https://doi.org/10.1016/j.ijbiomac.2017.09.044

[8] Yetria Rilda, Reza Safitri, Anthoni Agustien, Nasril Nazir, Achmad Syafiuddin, Hadi Nur, Enhancement of antibacterial capability of cotton textiles coated with TiO_2–SiO_2/chitosan using hydrophobization, *Journal of the Chinese Chemical Society*, 64, 11, (2017), 1347-1353 https://doi.org/10.1002/jccs.201700165

[9] Cai-Ling Ke, Fu-Sheng Deng, Chih-Yu Chuang, Ching-Hsuan Lin, Antimicrobial mechanisms and applications of chitosan and its derivatives, *Polymers*, 13, 6, (2021), 904 https://doi.org/10.3390/polym13060904

[10] Nabel A. Negm, Hassan H. H. Hefni, Ali A. A. Abd-Elaal, Emad A. Badr, Maram T. H. Abou Kana, Advancement on modification of chitosan biopolymer and its potential applications, *International Journal of Biological Macromolecules*, 152, (2020), 681-702 https://doi.org/10.1016/j.ijbiomac.2020.02.196

[11] Lisa N. Kasiewicz, Kathryn A. Whitehead, Recent advances in biomaterials for the treatment of diabetic foot ulcers, *Biomaterials Science*, 5, 10, (2017), 1962-1975 https://doi.org/10.1039/C7BM00264E

[12] Nadia Ahmed Mohamed, Mona Mohamed Fahmy, Synthesis and Antimicrobial Activity of Some Novel Cross-Linked Chitosan Hydrogels, *International Journal of Molecular Sciences*, 13, 9, (2012), 11194-11209 https://doi.org/10.3390/ijms130911194

[13] Jayachandran Venkatesan, Rangasamy Jayakumar, Annapoorna Mohandas, Ira Bhatnagar, Se-Kwon Kim, Antimicrobial Activity of Chitosan-Carbon Nanotube Hydrogels, *Materials*, 7, 5, (2014), 3946-3955 https://doi.org/10.3390/ma7053946

[14] Azadehsadat Hashemi Doulabi, Hamid Mirzadeh, Mohammad Imani, Nasrin Samadi, Chitosan/polyethylene glycol fumarate blend film: Physical and antibacterial properties, *Carbohydrate Polymers*, 92, 1, (2013), 48-56 https://doi.org/10.1016/j.carbpol.2012.09.002

[15] Anandrao R. Kulkarni, Vijaykumar I. Hukkeri, Hsing-Wen Sung, Hsiang-Fa Liang, A Novel Method for the Synthesis of the PEG-Crosslinked Chitosan with a pH-Independent Swelling Behavior, *Macromolecular Bioscience*, 5, 10, (2005), 925-928 https://doi.org/10.1002/mabi.200500048

[16] C. Godoy - Alcántar, Anatoly K. Yatsimirsky, J - M Lehn, Structure - stability correlations for imine formation in aqueous solution, *Journal of Physical Organic Chemistry*, 18, 10, (2005), 979-985 https://doi.org/10.1002/poc.941

[17] Renata Czechowska-Biskup, Radoslaw Wach, Janusz Rosiak, Piotr Ulanski, Procedure for determination of the molecular weight of chitosan by viscometry, *Progress on Chemistry and Application of Chitin and its Derivatives*, XXIII, (2018), 45-54

[18] Tanveer Ahmad Khan, Kok-Khiang Peh, Hung Seng Ch'ng, Reporting degree of deacetylation values of chitosan: The influence of analytical methods, *Journal of Pharmacy & Pharmaceutical Sciences*, 5, 3, (2002), 205-212

[19] Ming-Tsung Wu, Yen-Ling Tsai, Chih-Wei Chiu, Chih-Chia Cheng, Synthesis, characterization, and highly acid-resistant properties of crosslinking β-chitosan with polyamines for heavy metal ion adsorption, *RSC Advances*, 106, (2016), 104754-104762 https://doi.org/10.1039/C6RA21993D

[20] Hellen Franciane Gonçalves Barbosa, Maha Attjioui, Ana Paula Garcia Ferreira, Edward Ralph Dockal, Nour Eddine El Gueddari, Bruno M. Moerschbacher, Éder Tadeu Gomes Cavalheiro, Synthesis, Characterization and Biological Activities of Biopolymeric Schiff Bases Prepared with Chitosan and Salicylaldehydes and Their Pd(II) and Pt(II) Complexes, *Molecules*, 22, 11, (2017), 1987 https://doi.org/10.3390/molecules22111987

[21] Ismiyarto Ismiyarto, Sesika Novari, Ngadiwiyana Ngadiwiyana, Purbowatiningrum Ria Sarjono, Noor Basid Adiwibawa Prasetya, Modifikasi kain aktif

antibakteri berbasis komplek Mn(II) basa schiff kitosan–salisilaldehid, *Jurnal Penelitian Saintek*, 25, 1, (2020), 11-23 https://doi.org/10.21831/jps.v25i1.29821

[22] José E. dos Santos, Edward R. Dockal, Éder T. G. Cavalheiro, Synthesis and characterization of Schiff bases from chitosan and salicylaldehyde derivatives, *Carbohydrate Polymers*, 60, 3, (2005), 277-282 https://doi.org/10.1016/j.carbpol.2004.12.008

[23] Amritha Vijayan, A. Sabareeswaran, G. S. Vinod Kumar, PEG grafted chitosan scaffold for dual growth factor delivery for enhanced wound healing, *Scientific Reports*, 9, 1, (2019), 19165 https://doi.org/10.1038/s41598-019-55214-7

[24] Yongjun Tang, Zhigang Xue, Xingping Zhou, Xiaolin Xie, Chak-Yin Tang, Novel sulfonated polysulfone ion exchange membranes for ionic polymer–metal composite actuators, *Sensors and Actuators B: Chemical*, 202, (2014), 1164-1174 https://doi.org/10.1016/j.snb.2014.06.071

[25] Nita Kusumawati, Septiana Tania, Pembuatan dan uji kemampuan membran kitosan sebagai membran ultrafiltrasi untuk pemisahan zat warna rhodamin B, *Molekul*, 7, 1, (2012), 43 http://dx.doi.org/10.20884/1.jm.2012.7.1.105

[26] R. A. Lusiana, A. P. Saputry, N. B. Prasetya, Pengaruh sulfonasi terhadap karakteristik fisiko-kimia membran polisulfon, *Indonesian Journal of Mathematics and Natural Sciences*, 42, 1, (2019), 35-42

[27] Hamid Reza Mardani, Fatemeh Ravari, Askari Kalaki, Leila Hokmabadi, New Schiff-Base's Modified Chitosan: Synthesis, Characterization, Computational, Thermal Study and Comparison on Adsorption of Copper(II) and Nickel(II) Metal Ions in Aqueous, *Journal of Polymers and the Environment*, 28, 9, (2020), 2523-2538 https://doi.org/10.1007/s10924-020-01788-7

[28] Rohimmahtunnissa Azhar, Alfan Arbianto, Firdayani Firdayani, The Influence Study of The Mole Ratio Reactant in Ceftriaxone Sodium Synthesis Against The Yield of The Production, *International Journal of Innovation Engineering and Science Research*, 2, 8, (2018), 21-25

[29] Lakia Monique Champagne, The synthesis of water soluble n-acyl chitosan derivatives for characterization as antibacterial agents, LSU Doctoral Dissertations, 2008

[30] Heather A. Friedel, Deborah M. Campoli-Richards, Karen L. Goa, Sultamicillin, *Drugs*, 37, 4, (1989), 491-522 https://doi.org/10.2165/00003495-198937040-00005

[31] R. Selwin Joseyphus, M. Sivasankaran Nair, Antibacterial and Antifungal Studies on Some Schiff Base Complexes of Zinc(II), *Mycobiology*, 36, 2, (2008), 93-98 https://doi.org/10.4489/MYCO.2008.36.2.093

[32] Suzan A. Matar, Wamidh H. Talib, Mohammad S. Mustafa, Mohammad S. Mubarak, Murad A. AlDamen, Synthesis, characterization, and antimicrobial activity of schiff bases derived from benzaldehydes and 3,3′-diaminodipropylamine, *Arabian Journal of Chemistry*, 8, 6, (2012), 850-857 https://doi.org/10.1016/j.arabjc.2012.12.039

[33] Claudia M. Alonzo-de la Rosa, Francesco Copes, Pascale Chevallier, Jonnathan G. Santillán-Benitez, Georgina Carbajal-de la Torre, Diego Mantovani, Miriam V. Flores-Merino, Synthesis and characterization of a polymeric network made of polyethylene glycol and chitosan as a treatment with antibacterial properties for skin wounds, *Journal of Biomaterials Applications*, 35, 2, (2020), 274-286 https://doi.org/10.1177/0885328220922384

[34] Elbadawy A. Kamoun, El-Refaie S. Kenawy, Xin Chen, A review on polymeric hydrogel membranes for wound dressing applications: PVA-based hydrogel dressings, *Journal of Advanced Research*, 8, 3, (2017), 217-233 https://doi.org/10.1016/j.jare.2017.01.005

[35] Colin Kleanthous, Judith P. Armitage, The bacterial cell envelope, *Philosophical Transactions of the Royal Society B: Biological Sciences*, 370, 1679, (2015), 20150019 https://doi.org/10.1098/rstb.2015.0019

[36] Samuel I. Miller, Nina R. Salama, The gram-negative bacterial periplasm: Size matters, *PLOS Biology*, 16, 1, (2018), e2004935 https://doi.org/10.1371/journal.pbio.2004935